Looking at Localized Excitons in Quantum Structures: A Theoretical Description

O. Di Stefano[1]), S. Savasta, G. Martino, and R. Girlanda

Dipartimento di Fisica della Materia e Tecnologie Fisiche Avanzate, Universitá di Messina, Salita Sperone 31, 98166 Messina, Italy

We present a theory of scanning local optical spectroscopy in quantum structures taking into account structural disorder. The calculated spatially resolved spectra show the individual spectral lines from the exciton states localized by the disordered potential as well as the quasicontinua spectra at positions close to the potential barriers in agreement with the experimental findings.

Static structural disorder on mesoscopic length scale is an unavoidable feature of low-dimensional semiconductor structures such as quantum wells (QWs) and quantum wires (QWRs). These structures exhibit, in addition to the impurities, lattice imperfections, etc., which are also present in homogeneous bulk crystals, interface imperfections which can involve different components with different length scales. Disorder in these quantum structures results in an effective 2D (QWs) or 1D (QWRs) potential with spatial correlation which tends to localize the center of mass motion of excitons. The optical spectra of semiconductor nanostructures, which near the absorption edges are dominated by excitons, yield valuable information on the quality of the interfaces and the growth process [1, 2]. In order to investigate in detail the optical properties and the effects of disorder on the individual electronic quantum states, optical probes combining very high spatial and spectral resolutions are required [3–6].

Theoretical approaches modeling the interaction of quantum structures with highly inhomogeneous light fields have been recently presented [7–13]. Here we present theoretical calculations of local optical spectroscopy in QWs and in QWRs taking into account structural disorder. Excitons, produced by a low-optical excitation behave as an effective quantum particle of mass M whose wave-function runs at mesoscopic dimensions over many atomic units. These calculations show how local optical probes can partially map these mesoscopic wave-functions. The theoretical calculations consist of two steps in close analogy with real experiments. The first step is the *growth* of the sample. Each sample corresponds to a single realization of disorder with prescribed statistical properties. Once obtained the samples, we calculate the spectra, each spectrum obtained with the probe tip fixed at a point on the QW plane or along the wire free axis is a single complete calculation.

In reasonable good quality structures, the amplitudes of the confinement energy fluctuations are typically one order of magnitude smaller than the binding energy of the 1S exciton [14]. In this limit the relative exciton motion described by the effective wave-function $\phi_{1S}(\rho_{eh})$ may be assumed undistorted by disorder. So disorder affects signifi-

[1]) Corresponding author; Tel.: +39 090 6765393; Fax: +39 090 391382;
e-mail: distef@ortica.unime.it

cantly only the centre of mass (COM) motion through an effective potential $V(\mathbf{r})$. In the following we describe the highly inhomogeneous light field by assuming a Gaussian profile $g_{\mathbf{R}}(\mathbf{r})$ centered around the beam position $\mathbf{R}$. The total absorption under local illumination is proportional to [10–12]

$$\alpha_g(\mathbf{R},\omega) \propto \mathrm{Im}\,\langle g_{\mathbf{R}}|[\omega - i\delta - \hat{H}]^{-1}|\, g_{\mathbf{R}}\rangle\,, \tag{1}$$

where the Hamiltonian $\hat{H}$ describes the exciton COM motion and, in the coordinate representation, is given by $\hat{H}_{\mathbf{r}} = -(\hbar^2/2M)\nabla^2 + V(\mathbf{r}) + \hbar\omega_0$, where $\hbar\omega_0$ is the 1S exciton energy level in the ideal (disorder free) structure, $\mathbf{r}$ is the coordinate along the QW plane or the wire free axis, and $V(\mathbf{r})$ is the effective disorder potential felt by excitons. The degree of local information on the excitonic wave functions provided by $\alpha_g(\mathbf{R},\omega)$ is determined by the comparison between the scale of the spatial variations of the wavefunction and the spatial extension of the beam [10]. For example, for a spatially homogeneous light field, $\alpha_g(\mathbf{R},\omega)$ is proportional to the square modulus of the spatial integral of the excitonic wave function. For a infinitely narrow probe beam $\alpha_g(\mathbf{R},\omega)$ is proportional to the square modulus of the wavefunction calculated at $\mathbf{R}$. Although not direct, significative information on absorption under local illumination can also be obtained by subwavelength excitation spectroscopy [6, 15].

We model the random potential $V(\mathbf{r})$ felt by the excitons as a zero mean, Gauss distributed and spatially correlated process [16] defined by the property $\langle V(\mathbf{r})V(\mathbf{r}')\rangle = v_0^2\,\mathrm{e}^{-|\mathbf{r}-\mathbf{r}'|^2/2\xi^2}$, where $\langle\ldots\rangle$ denotes ensemble average over random configurations, v_0 is the width of the energy distribution, and ξ is the correlation length characterizing the potential fluctuations. This effective potential is a result of the convolution of the actual disorder potential felt by electrons and holes with the 1S exciton wave function $\phi(\rho_{\mathrm{eh}})$. In our simulation, after a single realization of disorder, the *growth* of the sample, calculations are carried out in real space mapping, on a fine mesh of points, $H_{\mathbf{r}}$, which is then tridiagonalized by using the *Lanczos* algorithm starting from the normalized initial state $|g_{\mathbf{R}}\rangle$. The relevant spectrum comes from the inversion of the resolvent matrix $(\omega + i\delta - H)^{-1}$ which is very fast in the tridiagonal form of the Hamiltonian H [11]. For both the structures taken in examination, we adopt an exciton kinetic mass of $m = 0.25m_0$ typical for AlAs/GaAs quantum wells.

For calculations on QWRs we have considered a system size of $L = 6\,\mu$m which has been divided into $n = 3000$ steps, $\delta = 80\,\mu$eV.

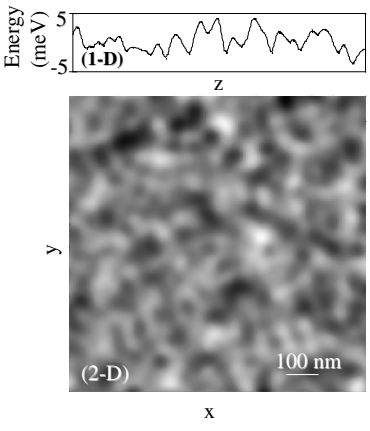

Fig. 1. Realizations of disorder potential with correlation length $\xi = 30$ nm for a QWR (1D) and a QW (2D)

Figure 1 (1D) displays the specific potential realization of the *sample* (in the investigated region) which has been obtained using the specific correlation length $\xi = 30$ nm and a strength $v_0 = 1.73$ meV. The calculations yield a two-dimensional matrix of data $\alpha_g(Z,\omega)$.

Figure 2 displays spatially resolved spectra $\alpha_g(Z,\omega)$, obtained by using beams with different spatial extension, as a function of photon energy ω

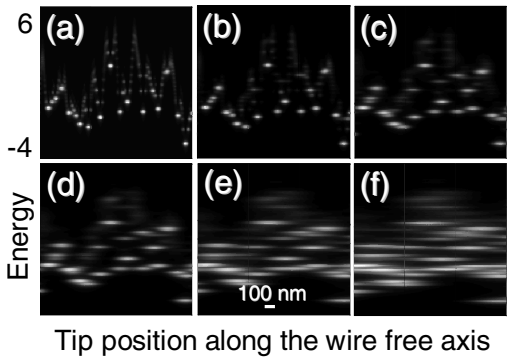

Fig. 2. Local absorption $\alpha_g(Z,\omega)$ as a function of beam position Z and photon energy along the free z-axis of the wire, obtained for the *sample* in Fig. 1 (1D)) and by using different spatial resolutions: a) $\sigma = 20$ nm, b) 40, c) 80, d) 120, e) 210, f) 300 nm. The line in the bottom of Fig. 3e measures 100 nm. The energy range on the vertical axis is between -4 and 6 meV for all the panels

and beam position Z along the free z-axis of the wire. At high spatial resolution (a, b) it is possible to observe sharp and spatially narrow structures from the individual eigenstates of the quantum system that provide detailed information on the spatial extension of the optically active quantum states. In agreement with experiments [17], we can observe at low energy structures fully localized inside only one potential well and, increasing the energy, extended structures arising from tunneling states between wells. Lowering spatial resolution the structures broaden, information on the potential profile is partially lost and, owing to the nonlocal character of light-matter interaction in semiconductors, cancellation effects can be observed due to destructive spatial interference of the corresponding quantum state [10, 12]. However we notice that, even when using a beam extension $\sigma = 300$ nm well beyond the spatial correlation of the disorder potential, a number of individual structures remain visible in agreement with experimental findings [5].

The local spectra in QWs have been calculated by considering a square region of 4 μm^2 which has been reproduced with a 500×500 mesh. Periodic boundary conditions have been adopted. For all the calculated spectra we used a homogeneous broadening $\delta = 60$ μeV. The calculations yield a three-dimensional matrix of data $\alpha_g(x,y,\omega)$. Figure 1 (2D) displays a 2D gray scale image of the region of the specific realized sample where local spectra have been calculated. The disordered potential has been obtained by using a correlation length $\xi = 30$ nm and a strength $v_0 = 1.5$ meV. Figure 3i displays a spectrum calculated with a beam with $\sigma = 250$ nm and centered in the middle of the windows in Fig. 1 (2D). Figures 3a–h show five 2D images generated by sectioning the data $\alpha_g(x,y,\omega)$ in planes of constant energy ω indicated by letters in Fig. 3i. The images, calculated using a beam with $\sigma = 40$ nm, show the different behaviour of two-dimensional excitons when varying the excitation energy and give information on the spatial extension of the quantum states which determine the sharp peaks in Fig. 3i. At low energy the images (Figs. 3a–e) display the lowest states of the exciton centre of mass motion located at the individual potential minima. Increasing the excitation energy, tunneling starts and we find an increasing number of structures which origin from excited states shared by different potential minima. An analogous behaviour has been observed in experimental spectroscopic images [3, 15].

In summary we have presented a theoretical formulation of scanning local optical spectroscopy in disordered quantum structures. We have performed calculations for a QWR and for a QW with interfacial roughness. We have reported calculations obtained for the specific disorder realization. We point out that the method presented here is

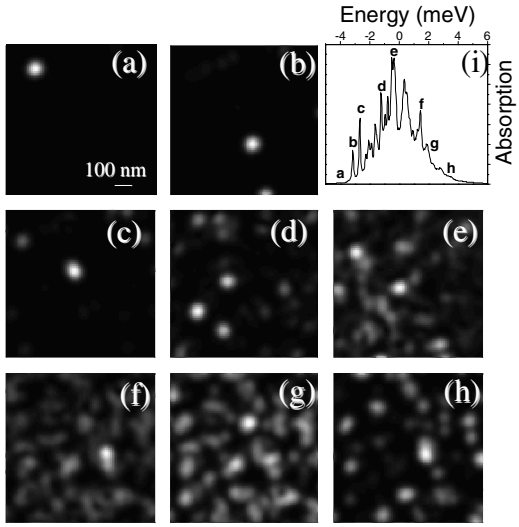

Fig. 3. a)–h) 2D images generated by sectioning the data $S_g^I(x, y, \omega)$ in planes of constant energy indicated by letters in Fig. 3i. i) Spectrum obtained using a Gaussian beam with $\sigma = 250$ nm centered in the middle of the image in Fig. 1 (2D)

general and can be applied for arbitrary disorder configurations. The images presented here show that our theoretical simulations can give a useful contribution to the interpretation of experimental investigations and characterizations. Furthermore the direct comparison of spectroscopic images with the realized disorder potential shown here, puts forward the correlation between structural disorder and spectroscopic near field images in QWs and QWRs. Moreover, these results have been obtained assuming that disorder does not perturb the e–h relative motion. This is not true in narrow quantum structures where this approximation becomes questionable. Work is in progress in order to relax this approximation and in order to include more realistic disorder potentials.

Acknowledgement We greatfully acknowledge useful discussions with V. Savona.

References

[1] C. Weisbuch, R. Dingle, A. C. Grossard, and W. Wiegmann, Solid State Commun. **37**, 219 (1981).
[2] M. A. Herman, D. Bimberg, and J. Christen, J. Appl. Phys. **70**, R1 (1991).
[3] H. F. Hess, E. Betzig, T. D. Harris, L. N. Pfeiffer, and K. W. West, Science **264**, 1740 (1994).
[4] A. Zrenner, L. V. Butov, M. Hagn, G. Abstreiter, G. Böhm, and G. Weinmann, Phys. Rev. Lett. **72**, 3382 (1994).
[5] J. Hasen, L. N. Pfeiffer, A. Pinczuk, S. He, K. W. West, and B. S. Dennis, Nature (London) **390**, 54 (1997).
[6] D. Gammon, E. S. Snow, B. V. Shanabrook, D. S. Katzer, and D. Park, Science **273**, 87 (1996); Phys. Rev. Lett. **76**, 3005 (1996).
[7] E. Runge and R. Zimmermann, phys. stat. sol. (b) **206**, 167 (1998).
[8] B. Hanewinkel, A. Knorr, P. Thomas, and S. W. Koch, Phys. Rev. B **55**, 13715 (1997).
[9] G. W. Bryant, Appl. Phys. Lett. **72**, 768 (1998).
[10] O. Mauritz, G. Goldoni, F. Rossi, and E. Molinari, Phys. Rev. Lett. **82**, 847 (1999); Phys. Rev. B **62**, 8204 (2000).
[11] S. Savasta, G. Martino, and R. Girlanda, Phys. Rev. B **61**, 13852 (2000).
[12] O. Di Stefano, S. Savasta, G. Martino, and R. Girlanda, Phys. Rev. B **62**, 11071 (2000).
[13] O. Di Stefano, S. Savasta, G. Martino, and R. Girlanda, Appl. Phys. Lett. **77**, 2804 (2000).
[14] R. F. Schnabel, R. Zimmermann, D. Bimberg, H. Nickel, R. Lösch, and W. Schlapp, Phys. Rev. B **46**, 9873 (1992).
[15] Q. Wu, R. D. Grober, D. Gammon, and D. S. Katzer, Phys. Rev. Lett. **83**, 2652 (1999).
[16] S. Glutsch and F. Bechstedt, Phys. Rev. B **50**, 7733 (1994).
[17] F. Intonti, V. Emiliani, C. Lienau, T. Elsaesser R. Nötzel and K. H. Ploog, Phys. Rev. B **63**, 075313 (2001).